ACCELERON AEROSPACE JOURNAL (AAJ)
E-ISSN: 2583-9942 (Online) | Accessible at www.acceleron.org.in
Volume 5, Issue 5, (pp.1585-1592)
Article ID: AAJ.11.2106-2562
Research Paper
https://doi.org/10.61359/11.2106-2562

Mean Aerodynamic Flow Field of an Impinging Jet Issuing from a Convergent Nozzle with Varying Nozzle to Plate Distance

Atri Bandyopadhyay[*1], Bharatkrishnan I[†2], Tapas Kumar Nag [‡2], Sanjoy Kumar Saha [§3], Dr.Prashant GK [**2]

[1] Department of Aerospace Engineering, Defense Institute of Advance Technology, DRDO, Girinagar, Pune Maharashtra-411025, India.

[2] Department of Aerospace Engineering, VIT Bhopal University, Kotri Kalan, Ashta, near Indore Road, Bhopal, Madhya Pradesh-466114, India.

[3] Aero-Entity, Vikram Sarabhai Space Centre, Thiruvananthapuram, Kerala-695022, India.

Abstract: Jet impinging on a flat surface draws a lot of attention among the researchers working in the area of aerodynamics not only because of its complex flow physics, but also due to its wide range of applications. Starting from launch vehicles during lift-off to aircraft during vertical take-off and landing, jets impinge on the surfaces (inclined as well as flat surface) has wide range of applications. Due to these impingements, high thermal and pressure loads acts on the surface where jets are impinging. Besides these high acoustic levels as well as loss of lift also generates during this impingement. Numerical flow simulations are carried out using commercial CFD code to understand the flow physics of an impinging jet on a flat surface. Simulations are carried out at a nozzle pressure ratio of 5.0 with varying distance between the nozzle to plate. The results so obtained are analyzed in detail and are brought out in this paper.

Table of Contents

1. Introduction

High-speed jet impinging on the surface can be found in a variety of aerospace-related applications. Lot of applications are found where jets interact with solid surfaces, for example jet impingement on launch pedestal during take-off and landing of aircraft, take off of launch vehicle, thrust vector control of nozzle, turbine cooling or aircraft engine exhaust interaction with solid airframes nearby etc. These jet flows are particularly troublesome to short take off and vertical landing (STOVL) aircraft, such the Harrier/AV-8 family, during hover mode. In these instances, the flow field produced by the impingement of the high-speed lift jets produces adverse local flow conditions, which can potentially lead to the degradation of aircraft performance in a number of areas during hover. These adverse effects, collectively referred to as ground effects, are the result of the highly unsteady nature of the flow generated by the impingement of the high-speed jet(s) on the ground plane and the pressure field caused by the natural entrainment by these jets. They include lift loss caused by flow entrainment associated with the lifting jets, which induces low surface pressures on the airframe resulting in a "suckdown" force opposite to lift. The lift loss typically increases in magnitude as the aircraft approaches the ground and can be greater than 60% of the total lift jet thrust when the jets are very close to the ground plane [1]. Increased noise or overall sound-pressure levels associated with high-speed impinging jets and the sonic fatigue of structural elements in the vicinity of the nozzle exhaust caused by unsteady loading is also an area of concern. In addition to higher noise levels, the noise spectrums are dominated by discrete tones, which, if close to the aircraft panel frequencies, can further aggravate the sonic fatigue problem. Furthermore, the impingement of hot, high-speed jets on the landing surface can lead to significant erosion caused by the extremely high shear stresses and wall heat-transfer rates created in this flow. Finally, due to hot gas ingestion, the outwash from the hot impinging jets can be drawn into the engine inlets. This will degrade the engine performance and can lead to engine failure. For the future generation of the supersonic STOVL aircraft, the environment is expected to be more severe because of the impingement of supersonic jets operating at higher temperatures. Consequently, the study of supersonic impinging jet flows is of great interest from a practical perspective. Furthermore, the complex nature of the impinging jet flow field, which

[*]Department of Aerospace Engineering, Defense Institute of Advance Technology, DRDO, Girinagar, Pune Maharashtra-411025, India. **Corresponding Author:** bandtintin@gmail.com.
[†]Department of Aerospace Engineering, VIT Bhopal University, Kotri Kalan, Ashta, near Indore Road, Bhopal, Madhya Pradesh-466114, India.
[‡]Department of Aerospace Engineering, VIT Bhopal University, Kotri Kalan, Ashta, near Indore Road, Bhopal, Madhya Pradesh-466114, India.
[§]Aero-Entity, Vikram Sarabhai Space Centre, Thiruvananthapuram, Kerala-695022, India.
[**]Program Chair, Department of Aerospace Engineering, VIT Bhopal University, Kotri Kalan, Ashta, near Indore Road, Bhopal, Madhya Pradesh-466114, India.
Article History: Received: 15-November-2025 || Revised: 29-November-2025 || Accepted: 29-November-2025 || Published Online: 30-November-2025.

often includes multiple shock and shock/shear layer interactions, subsonic, supersonic and separated flows (Figure 1), makes this flow very interesting for fluid dynamics aspect. Impinging jet flows have been the focus of research for over few decades, where their fluid dynamic and acoustic properties have been carefully examined by a number of investigators either numerically or experimentally. Some of them are Neuwerth [2] Powell [3] Tam and Ahuja [4] Henderson and Powell [5] and most recently Krothapalli et al [1].`

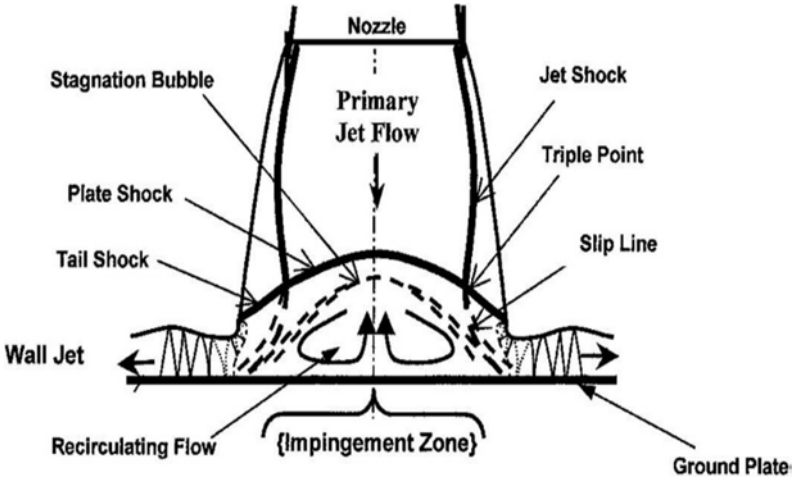

Figure 1: Schematic of the flow phenomena for normal impinging jet [9]

One of the primary findings of these aeroacoustics studies is that the impinging jet is highly unsteady and oscillatory in nature. This is accompanied by discrete, high-amplitude acoustic tones, referred to as impingement tones which is caused by a feedback loop. This feedback mechanism was first described by Powell [6], [7]. Recently, Krothapalli et al. [1] has estimated the lift loss through wind tunnel test. As the focus of the present work is the mean behaviour of the impinging jet, a more detailed discussion of the unsteady properties is outside the scope of this article though the fluid dynamic and acoustic properties of this flow appear to be intimately related.

2. Review of Related Literature

To understand the complex flow field generated due to the impingement of jet, flow simulations are carried out for a convergent nozzle. Flow simulations are carried out for a normal impinging jet at NPR = 5.0 with varying distance between the nozzle exit and bottom plate (h/D). Commercial code ANSYS Fluent [8] is used for the flow simulations

2.1 Geometric details:

Nozzle geometry considered here is shown in Figure 2. This nozzle geometry is taken from the literature [9] where wind tunnel test data are available. Nozzle is a converging axisymmetric sonic nozzle with exit diameter (D) = 25.4mm. A plate that is fixed at the nozzle exit plane (known as lift-plate) is of 10D in diameter. The diameter of the bottom plate (also called impinging plate) where the jet impinges is 24D. The nozzle inlet is at a distance of 4D from the nozzle exit plane. The distance (h/D) between the nozzle exit plane and the impinging plate (bottom plate) has been varied from 2.0 to 8.0 at a step of 2.0. Some other important dimensional details of the simulated geometry along with the CFD domain is shown in Figure 2.

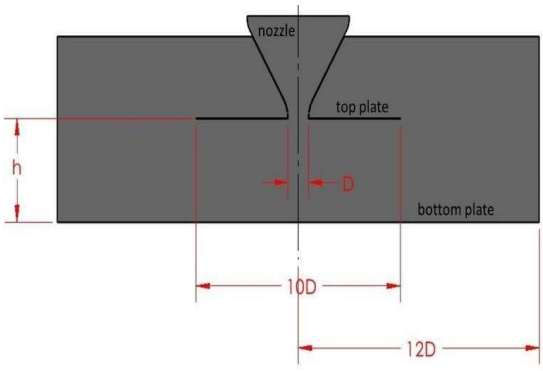

Figure 2: Dimensional details of the geometry

Acceleron Aerospace Journal || AAJ.11.2106-2562
Volume 5, Issue 5, pp (1585-1592)
E-ISSN- 2583-9942
https://dx.doi.org/10.61359/11.2106-2562

2.2 Domain and Grid

The objective of present study is to understand the mean flow physics of an impinging jet on a flat plate and its dependency of the nozzle to plate distance. As the nozzle is axisymmetric, domain considered for the simulations are of cylindrical in shape. Using the symmetricity of the body, $1/4^{th}$ of the complete body is used for simulation to reduce the computational cost. Grids of different dimensions are used across the simulation domain. Finest grids are used close to jet axis and coarsest one at the furthest point for the simulations. Before finalization of the grid distribution, grid independence studies are carried out. Based on this study, the grid sizes are finalised. A typical grid distribution is shown in Figure 3 for a typical case. Typical value of y+ is about 3.0. As we are mainly interested in the flow parameters beyond the nozzle exit and more-over the heat-flux or boundary layer is not studied here, the value of y+ is not so critical in this study.

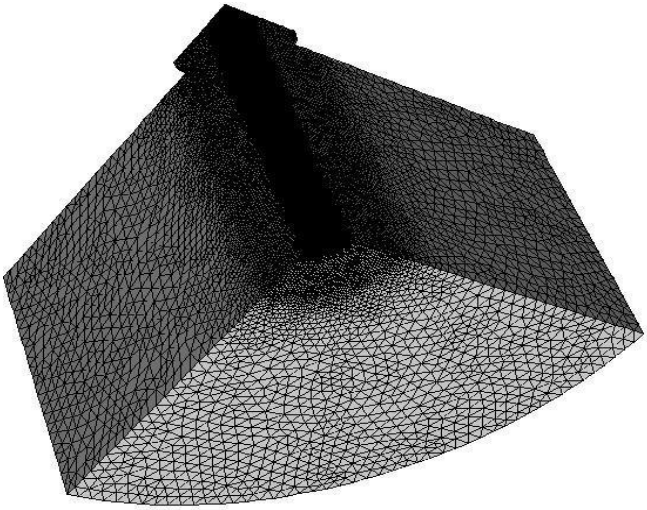

Figure 3: Grid distribution for h/D =4.0

2.3 Simulation parameter and boundary conditions

NPR value considered for the simulation is 5.0 which is same as the test. Ambient pressure considered for this simulation is 1bar (100000 pascal) and ambient temperature is 300K. Simulations are carried out for three different NPR values to cover the different jet profiles. Based on this and NPR values the stagnation pressure (P0) at the nozzle inlet is fixed at 5.0 bar(under-expanded) respectively. Total temp of air at inlet (T0) is 300 kelvin and air is considered as an ideal gas in this simulation.

Far field boundary condition is applied at the far field (12D away from the nozzle centre). As the exact thermal conditions about the plates (top and bottom plates) are not mentioned in the test report [9], adiabatic (T =300K), no-slip boundary conditions are applied in the simulations. No slip boundary condition is applied at nozzle also. At the inlet of the nozzle, pressure inlet condition is applied where total pressure (P0) and total temperature (T0) are specified. Symmetry conditions are applied at the symmetry planes of the domain.

3. Results and Discussion

It has earlier mentioned that commercial CFD code, ANSYS is used to simulate the flow. Pressure based coupled solver is used for the simulation where coupled algorithm solves a coupled system of equations comprising of the momentum and pressure equation. This is widely recommended by the different users of ANSYS and the governing equation for the conservation of mass, momentum and energy equations are discretized using a control volume-based technique. Based on earlier studies [10], RANS-based shear-stress transport (SST) k-x model was applied in the steady-state runs. Simulations are carried out till the residuals falls to 10-3 order and the variation in the central line fluid parameter does not vary more than 1%. As the impingement flow itself is unsteady by its nature and we are interested in the mean flow quantities, convergence of 10^{-3} is enough, no need to go for 10^{-6} order which will unnecessarily increase of the computational cost.

3.1 Validation of the data

Before proceeding for the detailed simulations, CFD results are compared with the test data available in the literature [9]. In Figure the numerical schlieren is compared with the schlieren available in literature. Two different instants are shown in Figure 4. It is noticed that the flow physics are nicely captured in CFD simulations.

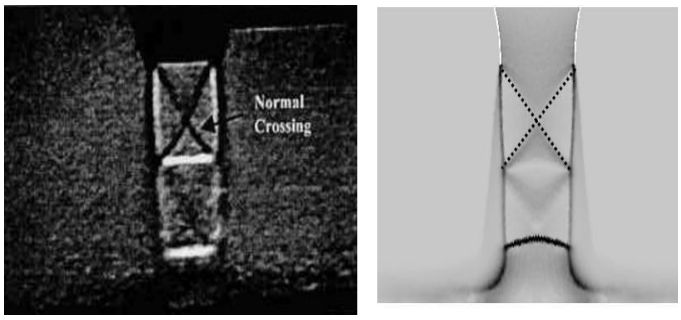

a) h/D = 2.0 at NPR = 2.5

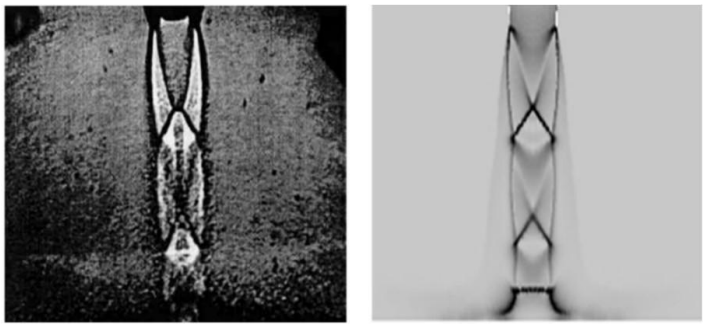

h/D = 4.0 at NPR = 3.7

Figure 4: Comparison of numerical and test schlieren

Variation of mean pressure value (Cp) along the radial direction of the bottom plate is estimated from the present simulations and plotted along with the literature data [9]. It is noticed that the pressure data so estimated also match well (Figure 5). Here Cp is non-dimensional surface pressure coefficients where, Cp

= (P – P∞)/ (P0 – P∞), similar as that was defined in literature [9]. This gives the confidence on the data so generated.

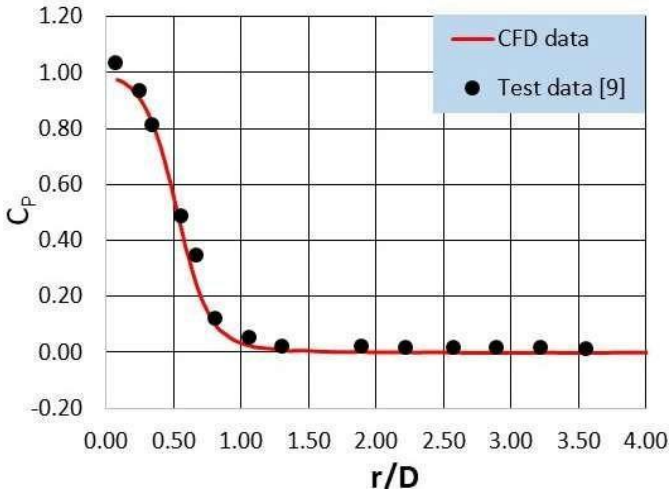

Figure 5: Cp Distribution (no top plate) at NPR=2.5

3.2 Mach palette

Earlier it has been mentioned that the nozzle considered here is a sonic nozzle where M=1.0 is expected at the exit plane irrespective of the nozzle inlet pressure (NPR). Mach number at the exit plane for all the simulated cases are checked for this consistence. Mach number variation along the radial direction is shown in Figure 6. It is noticed that Mach number at the nozzle exit is identical except very close to the nozzle wall. This may be due to the non-identical grid distribution and differences in boundary layer thickness at the nozzle exit (which is not captured here). The area average Mach number at the nozzle exit is ~1.0 as expected.

Acceleron Aerospace Journal || AAJ.11.2106-2562
Volume 5, Issue 5, pp (1585-1592)
E-ISSN- 2583-9942
https://dx.doi.org/10.61359/11.2106-2562

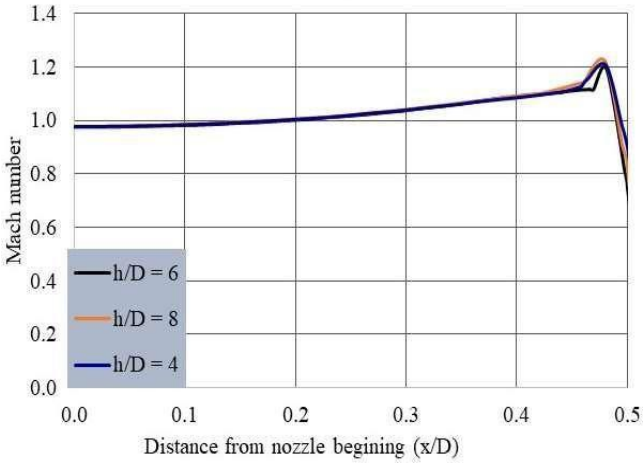

Figure 6: Mach number distribution along the nozzle exit plane

After coming out of the nozzle, the jet will expand (as this is a convergent nozzle) before the jet flow faces the bottom impinging plate. Due to the expansion, the pressure drops and gets compressed by shock. Based on the NPR values, the strength of expansion and compression depend. The nozzle is designed for an NPR =3.7. Hence, at NPR=5.0, the jet will plume, and its diameter will increase as soon as jet comes out of the nozzle. Due to this high expansion, there will be a Mach disc formation very close to the nozzle exit plane (Figure 7). This is noticed in all cases. It is noticed that the strength of the Mach disc is also similar across all the different cases studied. A normal shock (also called plate shock) is noticed near the bottom plate. Strength of this normal shock depends on the plate to nozzle distance(h/D). This is because, with the increase in distance, more amount of surrounding air gets mixed and reduces the strength of the main jet flow.

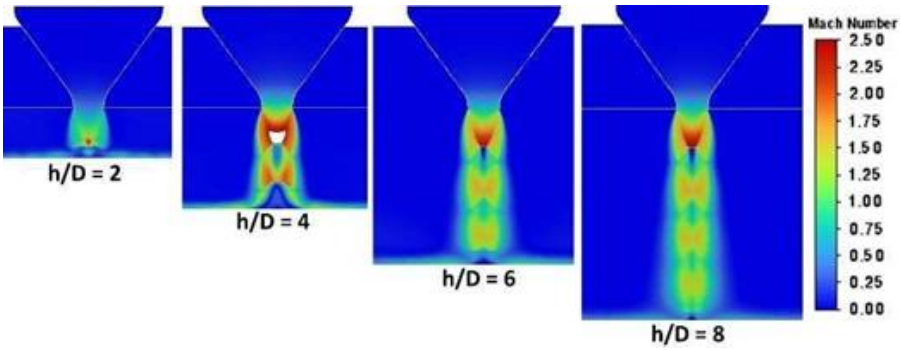

Figure 7: Mach number palette along the centre line

Numerical schlieren (density gradient) at different h/D are shown in Figure 8. Mach disc, barrel shock, plate shock etc. are clearly visible from it. Though Mach disc is formed for all the cases, for h/D=2.0 and 4.0, no shock cell is noticed due to the close proximity of the bottom plate. At higher h/D (6.0 and 8.0), the shock cells are clearly visible. It is interesting to note that the length of shock cell does not depend on the h/D values. This is similar to the observation reported in literature [11]. All this gives confidence on the correctness of the results obtained. Another interesting point to note that the width of the Mach disc is highest for h/D=2.0 and least for h/D=6.0 and 8.0. This is due to the influence of the bottom plate and shock generated due to the presence of the plate. The shape of the plate shock is different for different h/D values because of the mutual interaction of the plate shock with the Mach disc formed

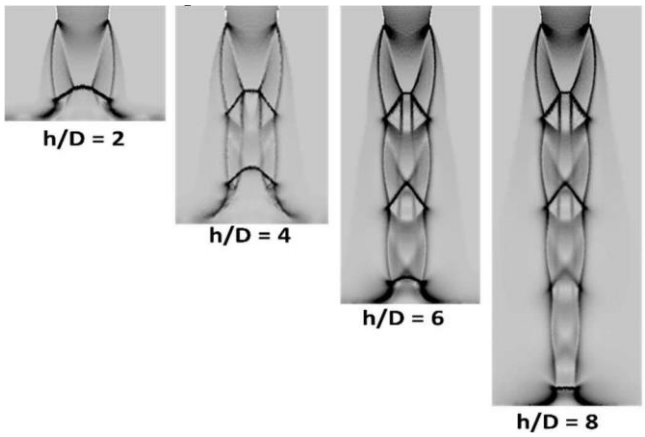

Figure 8: Numerical schlieren

3.3 Pressure palette

Earlier it was mentioned that shocks are formed once the flow comes out of the nozzle as the jet is under expanded. Numerous shock cells are formed based on the distance of the impingement plate. Another shock forms before the jet impinged on the bottom plate. Based on the distance of the impinging plate, the strength of the shock varies. This will lead to higher pressure on the plate. All these are clear from the pressure palette shown in Figure 9**.**

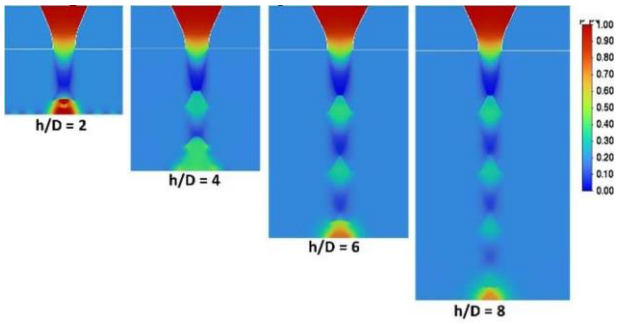

Figure 9: Pressure palette along the central line

Variation of pressure along the nozzle centre line is shown in Figure 10. Pressure fluctuation due to the formation of shock cell is clearly visible here. Number of shock cells, its length etc. are all clearly visible here. The sharp increase in pressure noticed at x/D = 5.3 is due to the formation of Mach disc. It is noticed that there will be a big, separated flow for lower h/D values (2 and 4), which is absent in other two cases. This is in- line with the literature data [12].

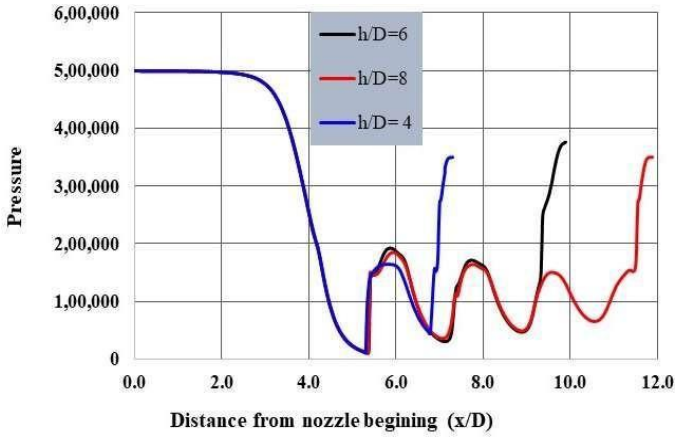

Figure 10: Pressure distribution along the nozzle centre line at NPR=5.0

Acceleron Aerospace Journal || AAJ.11.2106-2562
Volume 5, Issue 5, pp (1585-1592)
E-ISSN- 2583-9942
https://dx.doi.org/10.61359/11.2106-2562

3.4 Forces on the plates

Along with the jet flow, surrounding air gets entrained which will cause a reduction in the pressure at the bottom side of the plate located at the nozzle exit (top-plate). Whereas the top surface of the plate is unaltered. As a result, a downward force acts on the plate. The magnitude of this force varies depends on the distance between the impinging plate and nozzle. It is noticed that the amplitude of the force decreases exponentially with increasing the distance and with increase of NPR this value also increases. Similar work is carried out to estimate the forces on the bottom plate. With the increase of the distance of the impinging plate, the pressure value decreases. This will cause a reduction in the force on the bottom plate.

4. Conclusions

Steady state flow simulations are carried out using ANSYS Fluent to simulate the sonic impinging jet over a flat plate. Simulations are carried out for different jet pressure ratio and various nozzles to plate distance. It is noticed that as the NPR value increases, the shock cell length increases, and Maximum Mach number of the jet also increases. With the increase of h/D values, forces on the bottom plate reduces the lift-loss as well also decreases.

5. Acknowledgement

Authors want to express their gratitude to Mr. Anish who has helped to generate the geometry. Thanks to Dr Pankaj Priyadarshi, GD ADSG and Dr Patil, DD AERO for their support during the work.

6. Nomenclature

D	Exit diameter of the nozzle	[mm]
NPR	Nozzle Pressure Ratio i.e. ratio of the jet pressure at the nozzle exit plane to free stream pressure	--
M	Mach number of flow	--
P_0	Chamber pressure	[bar]
P	Local static pressure	[bar]
P_∞	Local free stream pressure	[bar]
h	Distance of the plate from the nozzle exit surface	[mm]
x	Distance measured from the nozzle inlet	[mm]

7. References

[1] Krothapalli, A., Rajkuperan, E., Alvi, F., & Lourenco, L. (1999). Flow field and noise characteristics of a supersonic impinging jet. Journal of Fluid Mechanics, 392, 155–181. https://doi.org/10.2514/6.1998-2239.
[2] Neuwerth, G. (1974). Acoustic feedback of subsonic and supersonic free jet which impinges on an obstacle. NASA TT F-15719.
[3] Powell, A. (1988). The sound-producing oscillations of round underexpanded jets impinging on normal plates. Journal of the Acoustical Society of America, 83, 515–533. https://doi.org/10.1121/1.396146.
[4] Tam, C. K. W., & Ahuja, K. K. (1990). Theoretical model of discrete tone generation by impinging jets. Journal of Fluid Mechanics, 214, 67–87. https://doi.org/10.1017/S0022112090000052.
[5] Henderson, B., & Powell, A. (1993). Experiments concerning tones produced by an axisymmetric choked jet impinging on flat plates. Journal of Sound and Vibration, 168, 307–326. https://doi.org/10.1006/jsvi.1993.1375.
[6] Powell, A. (1953a). On edge tones and associated phenomena. Acustica, 3, 233–243.
[7] Powell, A. (1953b). On the mechanism of choked jet noise. Proceedings of the Physical Society of London B, 66, 1039–1057. https://doi.org/ 10.1088/0370-1301/66/12/306.
[8] Ansys Fluent Theory Guide (2022 R1). (2022, January).
[9] Alvi, F. S., & Iyer, K. G. (1999, May). Mean and unsteady flow field properties of supersonic impinging jets with lift plates [AIAA Paper 99-1829]. https://doi.org/10.2514/6.1999-1829.
[10] Sanjoy, et al. (2022). Numerical prediction of mean flow characteristics of a supersonic jet issuing from a CD nozzle. In Proceedings of the 9th International and 49th National Conference on Fluid Mechanics and Fluid Power (pp. December 14-16, 2022). IIT Roorkee, Roorkee-247667, Uttarakhand, India.
[11] Wu, J., & New, T. H. (2019). Flow characterization of supersonic jets issuing from double-beveled nozzles. Journal of Fluids Engineering, 141(1), Article 011202. https://doi.org/10.1115/1.4040447.
[12] Kalghatgi, G. T., et al. (n.d.). The occurrence of stagnation bubbles in supersonic jet impingement flows. https://doi.org/10.1017/S0001925900007678.

8. Conflict of Interest

The author declares no competing conflict of interest.

9. Funding

No funding was issued for this research.